CHEMISTRY OF MATERIALS
Article

Chem. Mater. **2011,** *23,* 247–254 247
DOI:10.1021/cm102904f

Atomic Layer Deposition of Antimony and its Compounds Using Dechlorosilylation Reactions of Tris(triethylsilyl)antimony

Viljami Pore,*[,†,§] Kjell Knapas,[†] Timo Hatanpää,[†] Tiina Sarnet,[†] Marianna Kemell,[†] Mikko Ritala,[†] Markku Leskelä,[†] and Kenichiro Mizohata[‡]

[†]*Department of Chemistry, University of Helsinki, P.O. Box 55, FI-00014 University of Helsinki, Finland, and* [‡]*Accelerator Laboratory, Department of Physics, University of Helsinki, P.O. Box 43, FI-00014 University of Helsinki, Finland.* [§]*Current address: ASM Microchemistry Oy, Väinö Auerin katu 12 A, 00560 Helsinki, Finland.*

Received October 8, 2010

For the first time an element other than a metal was deposited by atomic layer deposition (ALD). Pure and conformal thin films of elemental antimony were prepared by ALD using $SbCl_3$ and $(Et_3Si)_3Sb$ as precursors. In situ reaction mechanism studies showed that the dehalosilylation reactions involved are very efficient in eliminating the ligands from the growing surface enabling the use of low growth temperatures down to 95 °C. Various antimony compounds, such as GeSb, Sb_2Te, GaSb, and AlSb, can also be deposited by reacting $(Et_3Si)_3Sb$ with other metal halides or mixing Sb growth cycles with other ALD processes. The new antimony ALD process is a major step in the realization of non-volatile phase change random access memories (PCRAM) and ALD of III−V compounds.

Introduction

Atomic layer deposition (ALD) is a unique modification of the Chemical Vapor Deposition method for highly controlled deposition of thin films.[1−3] Unique to ALD is that precursor vapors are brought onto the substrates alternately, one at a time, separated by purging periods with inert gas. The film grows via saturative surface reactions between the incoming precursor and the surface species left from the previous precursor. When all the reactions are saturative and no precursor decomposition takes place, the film growth is self-limiting providing a number of attractive features, such as easy and accurate film thickness control down to an atomic layer level, excellent large area uniformity, and unrivaled conformality on complex shaped substrates. These characteristics have made ALD the method of choice for the continuously downscaling microelectronics, and also for many other areas, in particular nanotechnology.[4,5]

The success of ALD is built on chemistry: for each material of an interest an appropriate combination of precursor molecules must be found that matches the ALD principle of alternate supply of precursors and reacts on the surface in the self-limiting manner without self-decomposition. With compound thin film materials it has been quite straightforward to find this kind of exchange reactions; a particularly universal approach for the growth of oxides, sulfides, and nitrides has been to exploit non-metal hydrides with various metal precursor compounds.[3] However, for elements such a universal chemistry does not exist at least for thermal ALD. With plasma enhanced ALD in principle all elements may be attempted using hydrogen radicals as reducing agents, but at this point it is too early to say how universal this approach turns out.[6,7] With thermal ALD, noble metals have been deposited using O_2 as the other precursor together with metal−organic and organometallic noble metal compounds,[8−10] and W has been deposited by reducing WF_6 with silanes and boranes.[11] In addition, some other metals like Cu, Fe, Co, and Ni have been deposited with varying success using H_2 as the reducing agent.[12] In the area of metalloids and non-metals many attempts have been made toward ALD of silicon and germanium but no real success has been met yet.[1]

Recently, we reported the ALD of tellurides and selenides using alkylsilyls of tellurium and selenium and various halides as precursors.[13] This chemistry was found to work at very low temperatures below 100 °C, and this was

*To whom correspondence should be addressed. E-mail: viljami.pore@helsinki.fi; viljami.pore@asm.com.

(1) Leskelä, M.; Ritala, M. *Thin Solid Films* **2002**, *409*, 138.
(2) Ritala, M.; Leskelä, M. *Handbook of Thin Film Materials*; Nalwa, H. S., Ed.; Academic Press: San Diego, CA, 2002; Vol. *1*, pp 103−159.
(3) Ritala, M.; Niinistö, J. *Chemical Vapour Deposition: Precursors, Processes and Applications*; Jones, A. C., Hitchman, M. L., Eds.; Royal Society of Chemistry: Cambridge, U.K., 2009; Chapter 4, pp 158−206.
(4) Ritala, M.; Niinistö, J. *ECS Trans.* **2009**, *25*, 641.
(5) Knez, M.; Nielsch, K.; Niinistö, L. *Adv. Mater.* **2007**, *19*, 3425.
(6) Rossnagel, S. M.; Sherman, A.; Turner, F. *J. Vac. Sci. Technol. B* **2000**, *18*, 2016.
(7) Lee, Y. J.; Kang, S.-W. *J. Vac. Sci. Technol. A* **2002**, *20*, 1983.
(8) Aaltonen, T.; Alén, P.; Ritala, M.; Leskelä, M. *Chem. Vap. Deposition* **2003**, *9*, 45.
(9) Aaltonen, T.; Ritala, M.; Sajavaara, T.; Keinonen, J.; Leskelä, M. *Chem. Mater.* **2003**, *15*, 1924.
(10) Aaltonen, T.; Ritala, M.; Sammelselg, V.; Leskelä, M. *J. Electrochem. Soc.* **2004**, *151*, G489.
(11) Klaus, J. W.; Ferro, S. J.; George, S. M. *Thin Solid Films* **2000**, *360*, 145.
(12) Lim, B. S.; Rahtu, A.; Gordon, R. G. *Nat. Mater.* **2003**, *2*, 749.
(13) Pore, V.; Hatanpää, T.; Ritala, M.; Leskelä, M. *J. Am. Chem. Soc.* **2009**, *131*, 3478.

Published on Web 12/17/2010

explained in terms of a favorable formation of alkylsilyl halides as volatile byproducts. In this article we report the low temperature deposition of elemental antimony exploiting similar dehalosilylation reactions between $(Et_3Si)_3Sb$ and $SbCl_3$. In addition, it will be shown that by combining the elemental antimony ALD process with the Sb_2Te_3, GeTe, and germanium antimony telluride (GST) phase change material (PCM) processes, one can widely expand the accessible compositions in the Ge−Sb−Te ternary system. This is of a great importance because crystallization rate and temperature, melting temperature, and electrical resistivities of the amorphous and crystalline states of the phase change material are all important factors which depend on the phase change material composition and affect the performance and data retention of PCM devices. Finally, the application of dehalosilylation chemistry on ALD of III−V antimonide compounds will be demonstrated.

Materials and Methods

Precursor Synthesis. $(Et_3Si)_3Sb$ was synthesized by reacting Na_3Sb with Et_3SiCl. Na_3Sb was prepared from the elements using naphthalene as a catalyst. Similar methods for preparing different alkyl silyl compounds of group 15 and 16 elements have been described in the literature.[14−16] All manipulations were done under rigorous exclusion of air and moisture using standard Schlenk and glovebox techniques. Hexane was deoxygenized by bubbling with Ar and dried and stored over 4 Å molecular sieves. Tetrahydrofuran (THF) was freshly distilled from sodium benzophenone ketyl. ^1H (200 MHz) and ^{13}C (50 MHz) NMR spectra were recorded with a Varian Gemini 2000 instrument at ambient temperature. Chemical shifts were referenced to $SiMe_4$ and are given in parts per million (ppm). The mass spectrum was recorded with a JEOL JMS-SX102 operating in electron impact mode (70 eV) using a direct insertion probe and a sublimation temperature range of 50−370 °C.

In a typical synthesis, 4.18 g (182 mmol) of Na cut in very thin slices, 7.38 g (61 mmol) of Sb powder, and 0.2 g of naphthalene were added into 200 mL of dimethoxyethane (DME) in a Schlenk bottle. The mixture was refluxed for 2 days and then cooled to room temperature. A 30.00 g portion (276 mmol) of Et_3SiCl was added, and the mixture was again refluxed for 2 days. DME was then evaporated, and 100 mL of hexane was added and the mixture was filtered with a Schlenk sinter. Hexane was evaporated off from the filtrate leaving a yellow-orange liquid. Yield: 22.28 g (77.5%) δ_H(200 MHz, $CDCl_3$) 0.84 (q, 18H, CH_2), 1.00 (t, 27H, CH_3); δ_C(50 MHz, $CDCl_3$) 9.17 ($SiCH_2$), 9.17 (CH_3). *m*/*z* (EI, 70 eV) 466 $[M]^+$, 437 $[(Et_3Si)_3Sb - Et]^+$, 409 $[(Et_3Si)_2SbSiEtH]^+$, 379 $[(Et_3Si)_2SbSi]^+$, 351 $[(Et_3Si)_2Sb]^+$, 322 $[(Et_3Si)_2Sb - Et]^+$, 319, 294 $[(Et_3Si)SbSiEtH]^+$, 266 $[(Et_3Si)SbSiH_2]^+$.

Film Deposition. The films were deposited onto 5×5 cm^2 native SiO_2/Si and soda lime glass substrates in flow-type F-120 ALD reactors (ASM Microchemistry Oy, Helsinki, Finland).[17] The ALD reactors were operated under a pressure of about 10 mbar using nitrogen (made on site by a Nitrox UHPN 3000 generator, rated purity of 99.9995%) as a carrier and purging gas. The precursors $SbCl_3$, $(Et_3Si)_3Sb$, $GeCl_2 \cdot C_4H_8O_2$, $GaCl_3$, and $AlCl_3$ were evaporated from open glass vessels inside the reactors at 30, 85, 65, 20, and 90 °C, respectively, and pulsed with inert gas valving.

Reaction Mechanism Studies. The in situ experiments were carried out at 98 °C in a specially modified F-120 reactor where the total area of the substrates was about 3500 cm^2.[18] The $SbCl_3$ pulses were usually 15 s long, the $(Et_3Si)_3Sb$ pulses 55 s long, and the purge periods 55 s long. Long pulse times were necessary to obtain stable QCM signals. Then also physisorption of excess precursor molecules occurred requiring long purge periods to desorb. The QMS was a Hiden HAL/3F 501 RC with a Faraday detector and an ionization energy of 70 eV. The pressure was reduced to about 1×10^{-5} mbar in the QMS chamber by differential pumping through a 100 μm orifice. The QCM was a Maxtek TM 400 with a sampling rate of 20 Hz.

From the QMS result that p% of the Et_3SiCl is released during the $SbCl_3$ pulse as compared to a complete ALD cycle, n is obtained as $3p/100$, since in reactions 2a−b (see below), a total of three Et_3SiCl molecules are released. From the QCM result m_1/m_0, n is obtained with molecular masses according to $m_0 = 2M(Sb) = 243.6$ and $m_1 = M(SbCl_3) - nM(Et_3SiCl) = 228.15 - 108.642n$, which give $m_1/m_0 = (228.15 - 108.642n)/243.6$ and further $n = (228.15 - 243.6\, m_1/m_0)/108.642$.

Film Characterization. The electron micrographs were obtained using a Hitachi S-4800 field emission scanning electron microscope. Film compositions were determined by using an INCA Energy 350 EDX spectrometer connected with the S-4800 and a GMR electron probe thin film microanalysis program.[19] Film crystallinity was examined with a PANalytical X′Pert Pro MPD X-ray diffractometer. For in situ X-ray diffraction (XRD) measurements an Anton-Paar HTK1200N oven was used. Film thicknesses were measured by X-ray reflection (XRR) using a Bruker D8 Advance X-ray diffractometer. Surface resistances were measured with a CPS four-point probe (Cascade Microtech Inc.) and a Keithley 2400 SourceMeter.

To analyze light impurities, time-of-flight elastic recoil detection analysis (TOF-ERDA) was carried out with a 5 MV tandem accelerator EGP-10-II using 48 MeV $^{79}Br^{9+}$ as a primary beam.[20] The results of the depth profiling should be regarded as only suggestive. The slopes and long tails in the Sb, Ge, and Si signals are not real, but generated by multiple scattering. As such the depth profiles can, however, be used to estimate whether the impurities reside at the interfaces or in the bulk of the film.

Preparation of Sb Nanotubes. Sb nanotubes were prepared at 100 °C using a porous alumina membrane (Whatman Anodisc) as the template. The membrane has pores of approximately 60 μm in length and 0.2 μm in diameter, giving an aspect ratio of 300:1. 1000 ALD cycles were applied with pulse lengths of 2 and 4 s for $SbCl_3$ and $(Et_3Si)_3Sb$, respectively, and 10 s purges for both. The alumina membrane was subsequently dissolved in 0.5 M KOH at 30−35 °C to give free-standing nanotubes of up to 10 μm in length. Even longer tubes would most likely be obtained by using longer pulse and purge times for the precursors.

Results

ALD of Elemental Antimony. Antimony, a Group 15 semimetal, has been widely used in lead batteries and as a dopant in the semiconductor industry, and it has also been

(14) Carmalt, C. J.; Steed, J. W. *Polyhedron* **2000**, *19*, 1639.
(15) von Hänisch, C. *Z. Anorg. Allg. Chem.* **2001**, *627*, 1414.
(16) Evans, C. M.; Castro, S. L.; Worman, J. J.; Raffaelle, R. P. *Chem. Mater.* **2008**, *20*, 5727.
(17) Suntola, T. *Thin Solid Films* **1992**, *216*, 84.
(18) Rahtu, A.; Ritala, M. *Electrochem. Soc. Proc.* **2000**, *2000−13*, 105.
(19) Waldo, R. A. *Microbeam Analysis: An Iteration Procedure to Calculate Film Compositions and Thicknesses in Electron-Probe Microanalysis*; San Francisco Press: San Francisco, CA, 1988; Vol. *23*, pp 310−314.
(20) Jokinen, J.; Keinonen, J.; Tikkanen, P.; Kuronen, A.; Ahlgren, T.; Nordlund, K. *Nucl. Instrum. Meth. B* **1996**, *119*, 533.

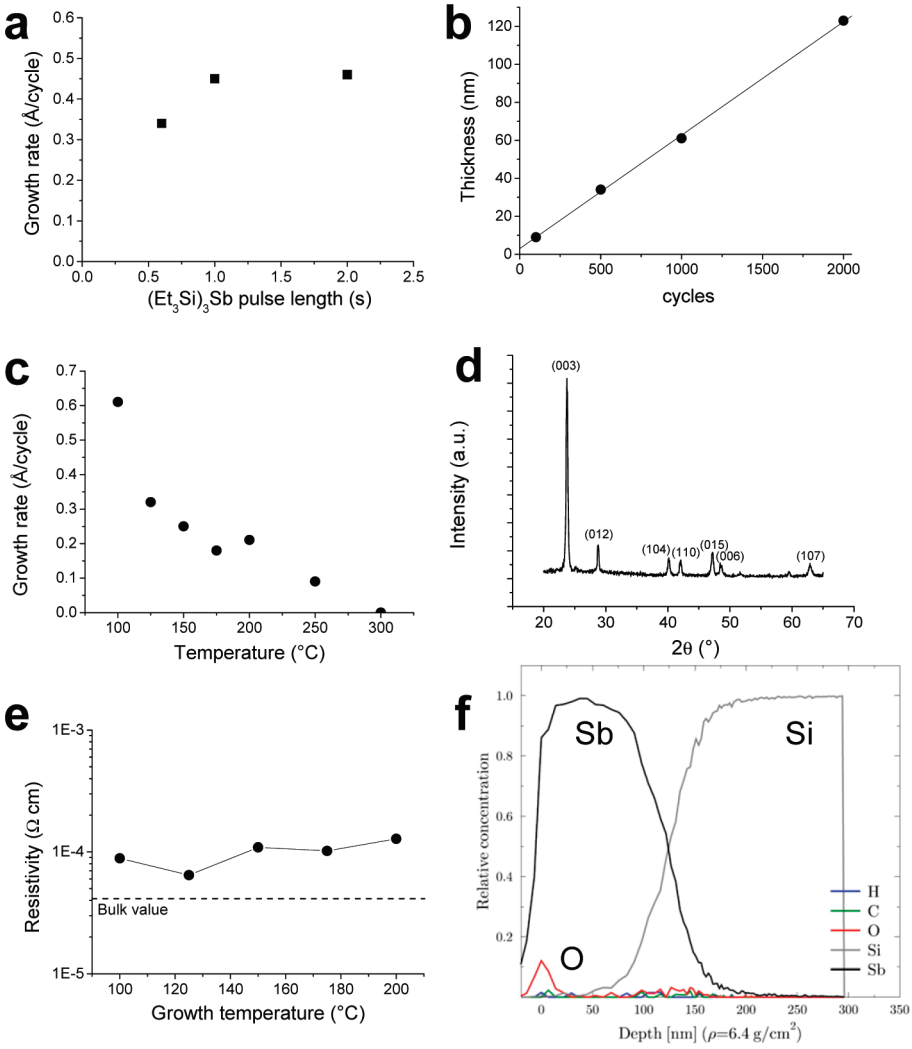

Figure 1. Characteristics of the $SbCl_3$-$(Et_3Si)_3Sb$ ALD process. (a) Growth rate of Sb films as a function of $(Et_3Si)_3Sb$ pulse length at 95 °C. (b) Sb film thickness as a function of the number of ALD cycles at 95 °C. (c) Growth rate of Sb films as a function of deposition temperature. (d) Grazing incidence XRD pattern of a Sb film prepared at 95 °C using 1000 ALD cycles. (e) Resistivity as a function of deposition temperature. (f) TOF-ERDA depth profile of a film grown at 100 °C.

studied as a pH electrode.[21,22] In thin film form Sb has been utilized as a lens material in super-resolution near-field structures (super-RENS) which may allow optical media with recording marks below the optical diffraction limit.[23]

Elemental Sb films were deposited in flow-type ALD reactors (F-120, ASM Microchemistry) using $SbCl_3$ and $(Et_3Si)_3Sb$ as the precursors. Soda lime glass and silicon with native oxide were used as the substrates. $(Et_3Si)_3Sb$ synthesized in house (see the Methods section) is a liquid at room temperature and was evaporated at 85 °C from an open boat inside the reactor. The evaporation temperature of $SbCl_3$ was 30 °C. Clear mirror-like films were produced at deposition temperatures of 95−250 °C. Figure 1a shows that at 95 °C the growth rate saturates to 0.45 Å/cycle at a $(Et_3Si)_3Sb$ pulse length of 1 s. The $SbCl_3$ pulse length was kept at 1 s, and all the purges were 2 s. The correlation between film thickness and number of deposition cycles was also linear, as seen in Figure 1b. As characteristic to ALD, the film growth is thus self-limiting, and the film thickness is dictated by the number of deposition cycles applied. FESEM images of the same films are shown in the Supporting Information, Figure S1. After 100 ALD cycles the film is not continuous but the nucleation density on native SiO_2/Si appears quite high. With larger number of ALD cycles continuous films are produced, and their roughness and grain size increase as a function of cycle number. Figure 1c shows that the growth rate decreases quite abruptly when the temperature is increased from 100 to 150 °C, stabilizes to ~0.2 Å/cycle at 150−200 °C, and then decreases again.[24] No film grew at

(21) Greenwood, N. N.; Earnshaw, A. *Chemistry of the Elements*, 2nd ed.; Butterworth-Heinemann: Oxford, 1998; pp 547−596.
(22) Opekun, A. R.; Smith, J. L.; Graham, Y. *Dig. Dis. Sci.* **1990**, *35*, 950.
(23) Tominaga, J.; Nakano, T.; Atoda, N. *Appl. Phys. Lett.* **1998**, *73*, 2078.

(24) There is a slight discrepancy between Figures 1a and 1b, 1c. The saturated growth rate in Figure 1a is 0.45 A/cycle whereas a growth rate of 0.61 Å/cycle is seen in Figures 1b and 1c at almost the same temperature. The reason for this difference is the high temperature dependence of the growth rate at the low temperature region (Figure 1c). We used different ALD reactors for the data in Figure 1a and Figures 1b,c. Small variations in the actual reactor temperatures are most likely responsible for these differences in the growth rates.

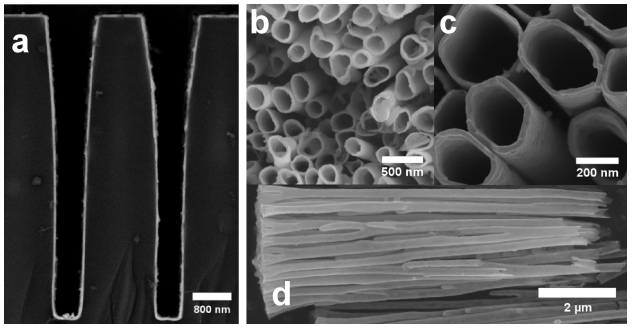

Figure 2. Conformality testing of the $SbCl_3$-$(Et_3Si)_3Sb$ ALD process. (a) Cross-section FESEM image of a Sb film deposited on a high aspect ratio trench structure. (b)−(d) FESEM images of Sb nanotubes prepared using a porous alumina membrane (Whatman Anodisc) as a template. The deposition temperature was 100 °C and amount of ALD cycles 1000. Pulse/purge lengths were 2/10 s for $SbCl_3$ and 4/10 s for $(Et_3Si)_3Sb$.

300 °C. FESEM images of Sb films grown at different temperatures are shown in the Supporting Information, Figure S2. Films prepared at 100 and 125 °C appear dense with few isolated grains on top. At 150−200 °C films start to appear slightly porous with voids between grains. At 250 °C only isolated grains are seen. The nucleation density thus appears to decrease when the temperature is increased. All the antimony films were polycrystalline (Figure 1d) with reflections identified as rhombohedral Sb.[25]

The resistivities of the films grown on soda lime glass were fairly close to the bulk values of Sb (41.7 $\mu\Omega$ cm).[21] Values between 60−100 $\mu\Omega$ cm were typically obtained with a four point probe. Figure 1e shows that the minimum in resistivity, 65 $\mu\Omega$ cm, occurred at a deposition temperature of 125 °C. The low resistivity values are reflected by the low impurity content measured by TOF-ERDA from a Sb film deposited at 100 °C. Chlorine was not detected at all, and the other impurity contents averaged over the whole film were H 0.6 ± 0.2, C 1.0 ± 0.2, and O 3.5 ± 0.3 at. %. As seen in the depth profile in Figure 1f, most of the oxygen was located in the interface regions, and more so at the film surface. The C and H impurities were concentrated in the film/substrate interface region. The contents of the impurities in the bulk of the film were thus exceptionally low, given the low deposition temperature of 100 °C.

The conformality of the new Sb process was studied by depositing an Sb film on a high aspect ratio trench structure at 100 °C. As seen in the cross-section FESEM image (Figure 2a) the film thickness appears the same in all areas of the test structure. Saturative film growth through self-limiting surface reactions, as characteristic to a good ALD process, is responsible for the observed excellent conformality. Sb nanotubes (Figures 2b−2d) were also prepared using template-directed deposition[26] with anodic alumina as the template that was removed after the Sb deposition (see the Methods section). The nanotubes were approximately 10 μm long and contained only minor amounts of impurities as judged by EDX (see Supporting Information, Figure S3). The new Sb process can thus be used to prepare various nanostructures by exploiting all the good qualities of ALD. It should also be pointed out that the low deposition temperature enables the use of many temperature sensitive materials such as polymers and biological materials as templates.

The growth mechanism of the Sb process was studied in situ at 98 °C with a quadrupole mass spectrometer (QMS) and a quartz crystal microbalance (QCM) integrated into a flow-type ALD reactor.[18] The volatile byproduct of the process was concluded to be Et_3SiCl similar to the $SbCl_3$-$(Et_3Si)_2Te$ and $GeCl_2 \cdot C_4H_8O_2$-$(Et_3Si)_2Te$ processes previously investigated with the same equipment.[27] Therefore the net reaction of the $SbCl_3$-$(Et_3Si)_3Sb$ ALD process depositing elemental antimony is a dehalosilylation reaction.

$$SbCl_3(g) + (Et_3Si)_3Sb(g) \rightarrow 2Sb(s) + 3Et_3SiCl(g) \quad (1)$$

This reaction also involves comproportionation of antimony. In a comproportionation reaction the same element is both oxidized and reduced so that on the reactant side the element exists at two oxidation states (in this case Sb^{+III} and Sb^{-III}) and on the product side at one (Sb^0) which is between the two oxidation states on the reactant side.

Similarly developing and about equally strong QMS signals at $m/z = 121$ (Et_2SiCl^+) and $m/z = 93$ ($HEtSiCl^+$), depicting the byproduct Et_3SiCl, were observed in the $SbCl_3$-$(Et_3Si)_3Sb$ process. The former was mainly used in the measurements that were aimed at quantifying how much byproduct is released at each step of an ALD cycle, an example of which is given in Figure 3a. The pattern displays a large and tall peak during the $SbCl_3$ pulse and a small and flat peak during the $(Et_3Si)_3Sb$ pulse, so Et_3SiCl is released during both precursor pulses but in greater amounts during the $SbCl_3$ pulse. If either of the precursors is pulsed repeatedly, no peak rises, so there are no interfering backgrounds. However, the $(Et_3Si)_3Sb$ pulse leaves the baseline a bit risen.

Comparison of the intensities of the peaks during the two different precursor pulses integrated from the baseline level indicates that (75 ± 7)% ($N = 34$) of Et_3SiCl is released during the $SbCl_3$ pulse as compared to a complete ALD cycle. However, there is a certain trend in the data; actually the mentioned fraction changes from (83 ± 5)% ($N = 11$) to (70 ± 4)% ($N = 20$) during a measurement session. The origin of this trend is discussed in more detail in the Supporting Information. The error limits are standard deviations, and N is the number of measurements.

Figure 3b shows QCM data of the process. During both precursor pulses the mass signal ascends and during both purge periods it descends to obtain a plateau. The descent during the purge periods is attributed to a desorption of physisorbed excess precursor molecules, cf. ref 27. The mass change after the $SbCl_3$ pulse and the following purge is denoted m_1, and the mass change after a complete ALD

(25) International Centre for Diffraction Data (ICDD), Card 35−0732.
(26) Bae, C.; Yoo, H.; Kim, S.; Lee, K.; Kim, J.; Sung, M. M.; Shin, H. *Chem. Mater.* **2008**, *20*, 756.
(27) Knapas, K.; Hatanpää, T.; Ritala, M.; Leskelä, M. *Chem. Mater.* **2010**, *22*, 1386.

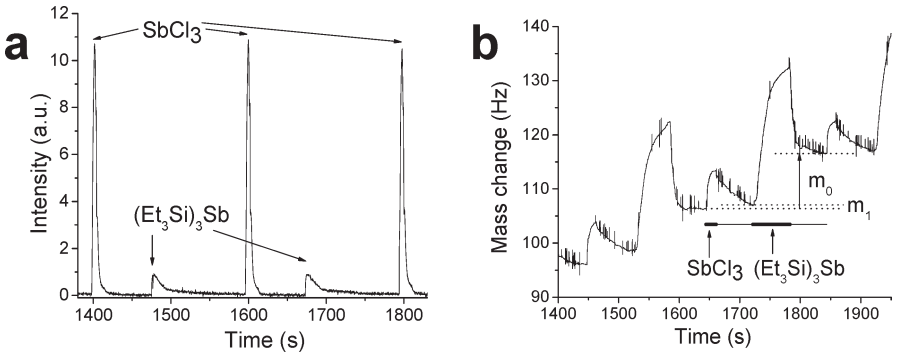

Figure 3. In situ reaction mechanism studies of the $SbCl_3$-$(Et_3Si)_3Sb$ ALD process. (a) QMS (m/z = 121, Et_2SiCl^+, fragment of Et_3SiCl) and (b) QCM results collected at a deposition temperature of 98 °C.

cycle m_0. As a result QCM gives that m_1/m_0 changes from -0.08 ± 0.19 ($N = 15$) to 0.27 ± 0.11 ($N = 18$) during a measurement session and is in average $0.11 \pm 0{,}23$ ($N = 33$). It was also verified that no net mass increase is observed with the QCM when either of the precursors is pulsed repeatedly, so no decomposition of the precursors occurs.

Because Et_3SiCl was the only gaseous byproduct detected, and it was found being released during both precursor pulses, the process must follow the exchange reactions 2a−b.

$$n - SiEt_3(s) + SbCl_3(g) \rightarrow - SbCl_{3-n}(s) + nEt_3SiCl(g) \quad (2a)$$

$$- SbCl_{3-n}(s) + (Et_3Si)_3Sb(g) \rightarrow 2Sb(s) + n - SiEt_3(s) + (3-n)Et_3SiCl(g) \quad (2b)$$

During the $SbCl_3$ pulse (eq 2a) the $SbCl_3$ molecules adsorb and react with the $-SiEt_3$ groups left on the surface after the previous $(Et_3Si)_3Sb$ pulse and converts the surface to chloride terminated. With QMS and QCM it is not possible to identify whether the $-SiEt_3$ (or $-Cl$) ligands are bonded to the same or different Sb atoms on the surface, for example, whether $=SbSiEt_3$ groups or $-Sb(SiEt_3)_2$ groups or both occur on the surface. The parameter n depicts the number of chloride ligands released, in average, from each adsorbing $SbCl_3$ molecule. Its value depends on the concentration of the $-SiEt_3$ groups on the surface. The remaining chloride ligands are eliminated during the following $(Et_3Si)_3Sb$ pulse (eq 2b), and thus the value of n does not bear any information about film contamination which arises from incompleteness of the reactions. The parameter n was determined independently from both the QMS and QCM results. According to QMS (QCM) n changes from 2.49 ± 0.14 (2.28 ± 0.43) to 2.10 ± 0.12 (1.49 ± 0.26) being in average 2.24 ± 0.22 (1.85 ± 0.53) (see the Methods section for derivations). QCM gives somewhat smaller values than QMS, but the QCM results also display greater deviations. The accentuated average of the averages according to QMS and QCM is $n = 2.13$, which is to be regarded as the final result best corresponding to practical growth experiments as far as we can tell.

ALD of Antimony Containing Phase Change Materials. Antimony is a constituent of many phase change materials Sb−Te, Ge−Sb, Ge−Sb−Te (GST), and Ag−In−Sb−Te (AIST) used in phase change random access memories (PCRAM, PCM) and CDs, DVDs, and Blu-ray discs.[28−33] PCM has recently gained interest as a potential memory technology beyond flash.[28−31] The operation of a PCM cell is based on the reversible phase change and the large resistivity difference between amorphous and crystalline states of the material. The switching in a phase-change memory cell is accomplished by heating the material locally with suitable current pulses which, depending on the intensity of the pulse, leave the material in a crystalline or amorphous state. Sputtering has usually been used in the deposition of PCM materials, but more conformal chemical deposition methods will be needed in the future when demanding 3-D pore-like cell structures will be utilized to reduce the programming current and minimize thermal crosstalk of the memory cells.[31] The thin film deposition methods must not only offer a good conformality but also a good control of the film composition. The following examples demonstrate how the current antimony ALD process adds a new dimension in tailoring the film composition of antimony containing phase change materials.

ALD of Sb−Te. In addition to the stoichiometric compound Sb_2Te_3, various other Sb−Te compositions, such as Sb_2Te, are important in PCM applications. The previously reported $SbCl_3$-$(Et_3Si)_2Te$ ALD process produces only stoichiometric Sb_2Te_3, without any possibility for composition control.[13] However, good composition control can be achieved when $(Et_3Si)_3Sb$ is used as a third precursor in the Sb−Te deposition process. To demonstrate this, Sb−Te films were grown by mixing Sb cycles ($SbCl_3$ + $(Et_3Si)_3Sb$) with Sb_2Te_3 cycles ($SbCl_3$ + $(Et_3Si)_2Te$) at a deposition temperature of 95 °C. Pulse lengths of 1 s were used for $SbCl_3$ and $(Et_3Si)_2Te$ and 2 s for $(Et_3Si)_3Sb$. The purge lengths were all 2 s. Figure 4a depicts the film composition as a function of $Sb_2Te_3/(Sb_2Te_3+Sb)$ cycle ratio. The compositions of pure Sb and Sb_2Te_3 are also indicated for clarity. It seems that there are two linear

(28) Ovshinsky, S. R. *Phys. Rev. Lett.* **1968**, *21*, 1450.
(29) Welnic, W.; Wuttig, M. *Mater. Today* **2008**, *11*, 20.
(30) Atwood, G. *Science* **2008**, *321*, 210.
(31) Lacaita, A. L. *Solid-State Electron.* **2006**, *50*, 24.
(32) Yamada, N.; Ohno, E.; Nishiuchi, K.; Akahira, N. *J. Appl. Phys.* **1991**, *69*, 2849.
(33) Matsunga, T.; Umetani, Y.; Yamada, N. *Phys. Rev. B* **2001**, *64*, 184116.

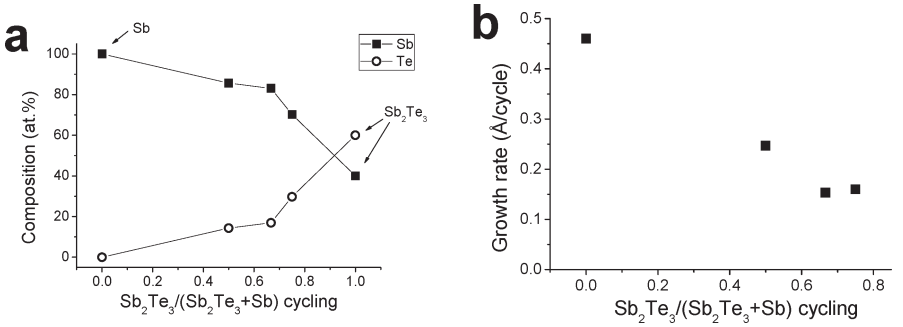

Figure 4. ALD of Sb−Te films. (a) Composition and (b) growth rate as a function of $Sb_2Te_3/(Sb_2Te_3+Sb)$ cycle ratio.

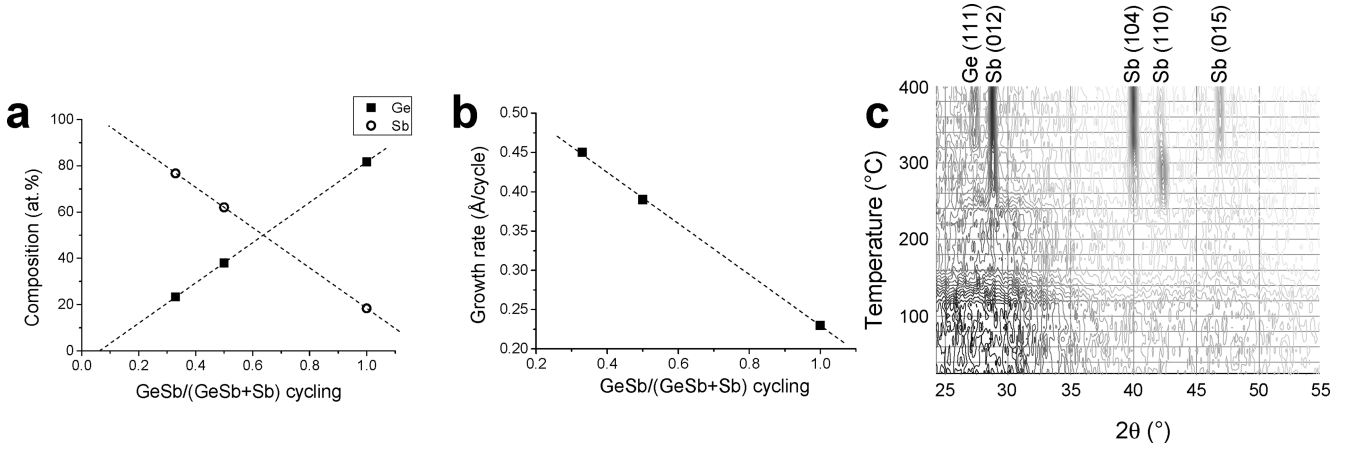

Figure 5. ALD of Ge−Sb films. (a) Composition and (b) growth rate as a function of GeSb/(GeSb+Sb) cycle ratio. The impurity contents were not taken into account in the composition plot. (c) HTXRD plot measured from a $Ge_{23}Sb_{77}$ film. All the Ge−Sb films were deposited at 95 °C using pulse/purge times of 4/6, 1/2 and 2/2 s for $GeCl_2 \cdot C_4H_8O_2$, $SbCl_3$, and $(Et_3Si)_3Sb$, respectively.

regions; a subtle change in composition up to a cycle ratio of 0.66 and then a more pronounced one from 0.66 to 1. It is clear that Sb−Te films with varying compositions can be prepared using ALD by adjusting the cycle ratio. Figure 4b shows the dependence of the growth rate on the cycle ratio. The growth rate seems to saturate to 0.15 Å/cycle with cycle ratios of 0.66 or higher. The growth rate of Sb_2Te_3 is not shown here, but it should be around 0.15 Å/cycle as well at this temperature.[13] All the Sb−Te films were crystalline showing a similar rhombohedral structure as pure Sb (Supporting Information, Figure S4) and no chlorine could be detected by EDX.

ALD of Ge−Sb. Ge−Sb, especially with the eutectic composition $Ge_{15}Sb_{85}$, is an important tellurium free PCM material.[34] It has a relatively high crystallization temperature making it suitable for memory applications where data retention at elevated temperatures is required. By exploiting the new Sb ALD process, Ge−Sb films with varying compositions were grown by ALD using $GeCl_2 \cdot C_4H_8O_2$, $(Et_3Si)_3Sb$, and $SbCl_3$ as precursors. When only $GeCl_2 \cdot C_4H_8O_2$ and $(Et_3Si)_3Sb$ were pulsed onto the substrate, a film with a composition of $Ge_{82}Sb_{18}$ was produced (Figure 5a). $GeCl_2 \cdot C_4H_8O_2$ and $(Et_3Si)_3Sb$ thus react with each other. When Sb cycles ($(Et_3Si)_3Sb + SbCl_3$) were mixed with the GeSb cycles ($GeCl_2 \cdot C_4H_8O_2 + (Et_3Si)_3Sb$), the composition could be accurately controlled as seen in Figure 5a. The dependence of the growth rate on the GeSb/(GeSb+Sb) cycling ratio was linear (Figure 5b). Some chlorine impurities could be detected in the Ge−Sb films by EDX, and a clear trend was observed: the higher the GeSb/(GeSb+Sb) cycle ratio the higher the chlorine residue contents. This suggests that the chlorine originates from the Ge precursor and/or binds with Ge in the film. A more accurate impurity analysis using TOF-ERDA was conducted for a $Ge_{22}Sb_{78}$ film and opposed to the Sb film the impurities were found uniformly throughout the film (Supporting Information, Figure S5). The impurity contents were: H 3.2 ± 0.7, C 1.1 ± 0.2, O 9.1 ± 0.8, and Cl 1.0 ± 0.2 at. %. The chlorine content is not alarmingly high but considerable amounts of oxygen were found instead. Probably some oxidation had occurred when the film was exposed to air.

All the prepared Ge−Sb films were amorphous in the as-deposited state. The crystallization behavior of a $Ge_{23}Sb_{77}$ film was studied by high-temperature XRD (HTXRD) in a N_2 atmosphere (Figure 5c). Crystallization started around 250 °C with the appearance of Sb reflections.[25] At 325 °C weak Ge reflections began to appear indicating Ge precipitation.[35] These observations are consistent with literature on sputtered GeSb films of similar composition.[34]

ALD of Ge−Sb−Te. We have earlier reported the ALD of GeTe, Sb_2Te_3 and GST using halides of Ge and Sb and

(34) Raoux, S.; Cabral, C.; Krusin-Elbaum, L.; Jordan-Sweet, J. L.; Virwani, K.; Hitzbleck, M.; Salinga, M.; Madan, A.; Pinto, T. L. *J. Appl. Phys.* **2009**, *105*, 064918.

(35) International Centre for Diffraction Data (ICDD), Card 04−0545.

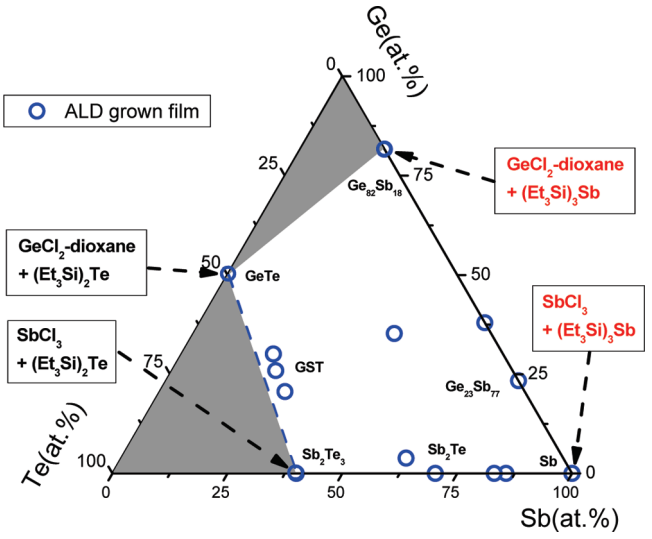

Figure 6. Ternary phase diagram for Ge, Sb, and Te. The white area indicates the compositions now accessible by ALD. Blue circles represent actual thin film samples prepared by ALD and measured by EDX. Impurities were left out from the composition assessment.

alkylsilyls of Te.[13] The composition of Ge−Sb−Te films prepared using these processes is, however, restricted only to the vicinity of the GeTe-Sb_2Te_3 tie line in the Ge−Sb−Te ternary phase diagram (Figure 6). Now, the use of $(Et_3Si)_3Sb$ as a precursor opens a large composition window in the phase diagram accessible to ALD. By mixing the four binary processes indicated in Figure 6 in appropriate ratios, films with any composition within the white area in the diagram can now be readily grown by ALD. Many important PCRAM materials lie within this composition range. To demonstrate the freedom to choose the stoichiometry, we deposited additional films with compositions $Ge_4Sb_{62}Te_{34}$ and $Ge_{35}Sb_{44}Te_{21}$ (Figure 6).

ALD of GaSb and AlSb. Antimony containing III−V semiconductors AlSb, GaSb, and InSb and their mixtures have various electronic and photonic device applications such as bipolar transistors, field effect transistors, lasers, and IR detectors.[36,37] Therefore it is of an interest to explore the applicability of the new $(Et_3Si)_3Sb$ precursor also for these materials. Indeed, also gallium chloride ($GaCl_3$) was found reactive toward $(Et_3Si)_3Sb$. Deposition experiments showed that films with a composition of roughly $GaSb_2$ were produced at 150 °C. Pulse length series of both $GaCl_3$ and $(Et_3Si)_3Sb$ indicated that the growth rate saturated to around 0.7 Å/cycle (Supporting Information, Figures S6 and S7). All the films were XRD amorphous as deposited. The films contained also some oxygen (approximated 5−15 at %) and chlorine (1−6 at %) impurities. Some oxidation of the films likely occurred after being exposed to ambient atmosphere as judged from the change of film appearance and the high oxygen content. These facts most likely caused the scatter seen in the data points in Supporting Information, Figures S6 and S7.

Preliminary studies have shown that $AlCl_3$ and $(Et_3Si)_3Sb$ react also resulting in films with an excess of Al. Most likely the excess Al is in the form of an oxide. The cubic AlSb phase[38] was, however, detected by XRD in a film deposited at 300 °C (Supporting Information, Figure S8). To our knowledge these are the first experimental results on the ALD of III−V antimonide compounds ever reported. Further improvement in film purity will be looked for by depositing the films in epitaxial form.

Discussion

Dehalosilylation reactions have been known already for quite some time.[39] This chemistry has been used to grow InP, GaAs, and InAs materials from solution at room temperature.[39−41] Also, many sulfides have been prepared from $(R_3Si)_2S$ and halide compounds.[42] The reactions are usually fast, highly exothermic, and clean with very little impurities found in the product. These are all interesting observations from the ALD point of view. For a successful ALD precursor combination, high reactivity is a key requirement[1−3] which many reported dehalosilylation reactions seem to meet. Other important ALD precursor requirements are sufficient volatility and thermal stability in the process temperature. So far, our experience in using alkylsilyls of Sb, Te, and Se in ALD indicates that these requirements are also met. It is rather the properties of the other reactant (i.e., halide) that may limit the use of dehalosilylation reactions in ALD in some cases.

The process for elemental antimony reported here is quite unique when compared to the other existing ALD processes for elemental thin films. Typically there is only one precursor compound containing the element to be deposited, and this compound is reacted with O_2, H_2, silane, or borane to eliminate the ligands. Here for the first time in ALD two different precursors bearing the same element, but with different oxidation states, were shown to result in clean ligand removal and deposition of elemental films through dehalosilylation that also involves comproportionation of the element being deposited. This is a fundamentally new approach for ALD which could work with elements other than antimony as well, provided that the right chemistries could be found. On the other hand, comproportionation is especially typical for the group 15 elements with reactions 3 and 4 being common textbook examples. In reaction 4 nitrogen undergoes exactly the same changes in oxidation states as antimony in reaction 1.

$$NH_4NO_3(s) \rightarrow N_2O(g) + 2H_2O(g) \quad (3)$$

$$NH_4NO_2(s) \rightarrow N_2(g) + 2H_2O(g) \quad (4)$$

The possibility to grow GaSb and AlSb films by ALD has been demonstrated for the first time. New types of devices based on these III−V materials can be envisaged where conformal films are required. We also predict that

(36) Dutta, P. S.; Bhat, H. L.; Kumar, V. *J. Appl. Phys.* **1997**, *81*, 5821.
(37) Dupuis, D. R. *Science* **1984**, *226*, 623.
(38) International Centre for Diffraction Data (ICDD), Card 06−0233.
(39) Wells, R. L.; Pitt, C. G.; McPhail, A. T.; Purdy, A. P.; Shafieezad, S.; Hallock, R. B. *Chem. Mater.* **1989**, *1*, 4.
(40) Micic, O. I.; Curtis, C. J.; Jones, K. M.; Sprague, J. R.; Nozik, A. J. *J. Phys. Chem.* **1994**, *98*, 4966.
(41) Cao, Y.; Banin, U. *J. Am. Chem. Soc.* **2000**, *122*, 9692.
(42) Martin, M. J.; Qiang, G.-H.; Schleich, D. M. *Inorg. Chem.* **1988**, *27*, 2804.

by using similar dehalosilylation chemistry as reported here, but for arsenic or phosphorus, low temperature ALD of other important III−V compounds such as GaAs or InP might be possible. Previously ALD of III−V compounds has been attempted using chemistry borrowed from MOCVD, that is, metal alkyl compounds reacting with non-metal hydrides.[43] In addition metal chlorides have been used as precursors.[44] The processes have not been very successful, and in many cases use of very high temperatures or plasma or laser assistance has been required. Interesting results have been obtained with *t*-butylarsine at temperatures near 400 °C or more though.[45,46] Conclusion on the earlier III−V ALD studies is not straightforward since all the papers are strictly focused on epitaxy. However, we believe that the dehalosilylation chemistry may open up a new era in III−V ALD chemistry.

Conclusions

We have shown that $(Et_3Si)_3Sb$ is reactive toward $SbCl_3$ and other metal chlorides at relatively low temperatures in ALD conditions. The control of Sb content in alloy films using the new $SbCl_3$-$(Et_3Si)_3Sb$ process allows plasma-free ALD growth of many phase change materials which were not previously possible. These include pure Sb, Sb_2Te, and $Ge_{15}Sb_{85}$, among others. Sb-rich GST materials, which were recently shown to exhibit polarity-dependent resistance switching, could also be prepared.[47] In addition, the ALD of III−V antimonides seems quite promising. The results presented here together with our earlier reported telluride and selenide ALD processes[13] offer a large selection of materials which can now be deposited conformally on demanding 3D structures. The use of efficient dehalosilylation reactions in ALD has opened up a great number of new possibilities.

Acknowledgment. We thank the Academy of Finland for financial support. The work in the Department of Chemistry, University of Helsinki, was done on an assignment of ASM Microchemistry Oy. Mr. Mikko Heikkilä is thanked for assistance with the HTXRD studies.

Supporting Information Available: Supporting discussion on the Sb film growth mechanism, FESEM images of Sb films, characterization of Sb nanotubes, XRD of Sb−Te and Al−Sb films, elemental depth profile of Ge−Sb and growth rate saturation of Ga−Sb. This material is available free of charge via the Internet at http://pubs.acs.org.

(43) Ozeki, M. *Mater. Sci. Rep.* **1992**, *8*, 97.
(44) Usui, A. *Proc. IEEE* **1992**, *80*, 1641.
(45) Chen, Q.; Beyler, C. A.; Dapkus, P. D.; Alwan, J. J.; Coleman, J. J. *Appl. Phys. Lett.* **1992**, *60*, 2418.
(46) Arès, R.; Watkins, S. P.; Yeo, P.; Horley, G. A.; O'Brien, P.; Jones, A. C. *J. Appl. Phys.* **1998**, *83*, 3390.
(47) Pandian, R.; Kooi, B. J.; Oosthoek, J. L. M.; van den Dool, P.; Palasantzas, G.; Pauza, A. *Appl. Phys. Lett.* **2009**, *95*, 252109.